

# PCCP

Accepted Manuscript



This is an *Accepted Manuscript*, which has been through the Royal Society of Chemistry peer review process and has been accepted for publication.

*Accepted Manuscripts* are published online shortly after acceptance, before technical editing, formatting and proof reading. Using this free service, authors can make their results available to the community, in citable form, before we publish the edited article. We will replace this *Accepted Manuscript* with the edited and formatted *Advance Article* as soon as it is available.

You can find more information about *Accepted Manuscripts* in the [Information for Authors](#).

Please note that technical editing may introduce minor changes to the text and/or graphics, which may alter content. The journal's standard [Terms & Conditions](#) and the [Ethical guidelines](#) still apply. In no event shall the Royal Society of Chemistry be held responsible for any errors or omissions in this *Accepted Manuscript* or any consequences arising from the use of any information it contains.

## Spin mixing at level anti-crossings in the rotating frame makes high-field SABRE feasible

Cite this: DOI: 10.1039/x0xx00000x

Andrey N. Pravdivtsev,<sup>a,b</sup> Alexandra V. Yurkovskaya,<sup>a,b</sup> Hans-Martin Vieth,<sup>c</sup> and Konstantin L. Ivanov<sup>a,b</sup>

Received 00th January 2012,

Accepted 00th January 2012

DOI: 10.1039/x0xx00000x

www.rsc.org/

A new technique is proposed to carry out Signal Amplification By Reversible Exchange (SABRE) experiments at high magnetic field. SABRE is a method, which utilizes spin order transfer from para-hydrogen to the spins of a substrate in transient complexes with suitable catalysts. Such a transfer of spin order is efficient at low magnetic fields, notably, at Level Anti-Crossing (LAC) regions. Here it is demonstrated that LAC conditions can also be fulfilled at high fields in the rotating reference frame under the action of an RF-field. Spin mixing at LACs allows one to polarize substrates at high fields as well; the achievable NMR enhancements are around 360 for the ortho-protons of partially deuterated pyridine used as a substrate and around 700 for H<sub>2</sub> and substrate in the active complex with the catalyst. High-field SABRE effects have also been found for several other molecules containing a nitrogen atom in the aromatic ring.

Signal Amplification By Reversible Exchange (SABRE) is a technique suggested in 2009<sup>1</sup> that has drawn considerable attention during the last few years<sup>2-9</sup>. The SABRE method, which is a variant of the Para-Hydrogen Induced Polarization (PHIP) technique<sup>10</sup>, is based on transfer of spin order from parahydrogen, which is the H<sub>2</sub> molecule in its singlet spin state, to a substrate in a transient complex with a suitable catalyst. As a result, the substrate gets hyperpolarized and its Nuclear Magnetic Resonance (NMR) signals are strongly enhanced. By using this method, molecules such as pyridine,<sup>1</sup> derivatives of pyridine and pyrazole<sup>5</sup>, as well as purine nucleotides<sup>9</sup> can be hyperpolarized. Since the SABRE technique does not require chemical modification of molecules, in contrast to the classical PHIP, which requires binding of H<sub>2</sub> to a substrate, it is potentially a more general method promising for many new NMR applications. Because of the cyclic character of the process SABRE makes continuous production of hyperpolarization<sup>9</sup> possible and enables measurements with nanomolar concentrations of substrate<sup>7</sup>. Signal enhancement provided by the SABRE method is often 2-3 orders of magnitude as compared to thermal NMR signals at high magnetic field. As there is high demand for signal enhancement in NMR the

SABRE method is extremely promising for utilization in NMR spectroscopy and imaging.

One of the problems with the SABRE technique is that it is most efficient at low fields, whereas in NMR spectroscopy it is advantageous to run measurements at high fields where the spectral resolution is much better. Thus, to perform high-resolution NMR studies with SABRE-derived hyperpolarization one needs to perform field-cycling, which can be technically difficult, and is also imposing limitations on the hyperpolarization lifetime. For practical purposes it is advantageous to polarize nuclear spins by SABRE directly at the high field of an NMR spectrometer or imager. In a recent paper Barskiy et al.<sup>8</sup> have shown that SABRE is manifest at high fields and signal enhancements of about 5 are achievable. In this case polarization of substrates is presumably due to cross-relaxation in the complex; the resulting spin polarization is orders of magnitude lower than at low fields, where spin order transfer is an efficient coherent process.

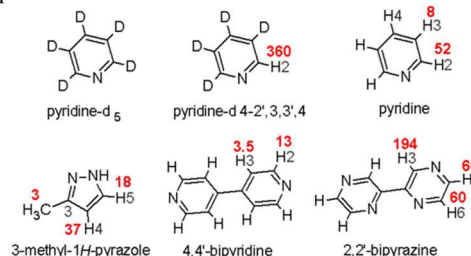
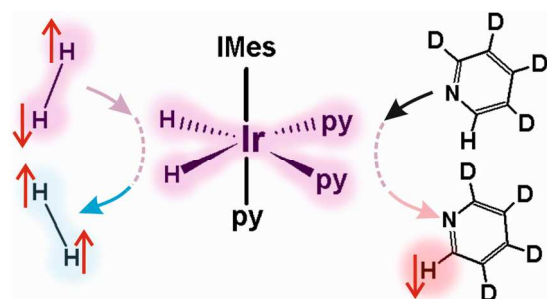


**Chart 1.** Chemical structures of substrates used; assignments of the proton positions and absolute values of the achieved NMR signal enhancements are also specified.

Here we present an approach, which makes efficient high-field SABRE feasible. The transfer of spin order is fast and provides NMR signal enhancements of up to 360 for free substrates and around 700 for protons of H<sub>2</sub> and of the substrate molecules bound to active catalysts. As the key idea we use the fact that polarization transfer, in general,<sup>11-16</sup> and for SABRE, in particular<sup>17</sup> is most efficient at nuclear spin Level Anti-Crossings (LACs) in the transient complex of parahydrogen, catalyst and substrate. Typically, such LACs are occurring<sup>17, 18</sup> at magnetic fields below 20-30 mT; nonetheless, the same ideas can be exploited when the spin system is brought to LACs in the rotating frame under the action of a strong

RF-field (spin-locking field). We will explain the physical principles behind this technique and present experimental results for high-field SABRE under spin-locking conditions, RF-SABRE. Advantages and potential applications of the method are also discussed.

SABRE-derived polarization was formed in complexes of several substrates, see Chart 1, with parahydrogen at two different catalysts: Crabtree's catalyst<sup>19</sup> and the recently proposed IrMes catalyst<sup>4</sup>. As an example the structure of the active complex of IrMes with partially deuterated py with a single *ortho*-proton, as well as the reaction pathway leading to the SABRE effect are shown in Scheme 1. Here, for the sake of simplicity, we will mostly discuss SABRE effects for deuterated pyridine (py) with the abundance of protons of only 0.5% so that the substrate contains only one proton or no protons at all. Further experiments with protonated py and other substrates are presented in Electronic Supplementary Information (ESI); in these systems the spin dynamics is more complex and NMR signal enhancements are lower. SABRE experiments were carried out at the high field of a 200 MHz spectrometer (magnetic field  $B_0=4.7$  Tesla) in the following way: First we let the system relax to its thermal equilibrium at  $B = B_0$ . After that the  $H_2$  gas enriched in its para-component (92% parahydrogen) is bubbled through the sample for 6 s. During this period the dihydrogen gas is efficiently dissolved in the sample. After waiting for 1.5 s, necessary to remove bubbles from the solution, an RF-field with amplitude  $v_1$  and frequency  $\nu_{rf}$  (spin-locking) is turned on for  $\tau_{rf}$ , which is varied in the range 0.1-7 s. The duration of the spin-locking period is long enough that complex formation and dissociation can frequently occur;  $\tau_{rf}$  is smaller than the relaxation time of the protons of free py and comparable to the relaxation time of the py protons in the active complex. We checked that the polarization level gets saturated for py at  $\tau_{rf} \approx 5$  s (while for the relaxation-based mechanism the saturation occurs after 100 s of bubbling<sup>8</sup>). When the parameters  $v_1$  and  $\nu_{rf}$  are set properly (see below), the substrate acquires hyperpolarization. Transverse spin magnetization (free induction) is seen immediately after switching off the RF-field. By taking the Fourier transform of the free induction decay we obtained NMR spectra with enhanced lines. If instead of transverse magnetization longitudinal magnetization is desired it is simple to generate it by applying a  $\pi/2$  pulse 90-degrees out-of-phase with respect to the spin-locking RF-field.



**Scheme 1.** SABRE formation in the complex of the IrMes catalyst with parahydrogen and partially deuterated pyridine (py) having only one proton in the *ortho*-position, IrMes=1,3-bis(2,4,6-trimethylphenyl) imidazole-2-ylidene. Transfer of the initial singlet spin order (represented by anti-parallel arrows) of the parahydrogen molecule entering the complex results in polarization of py (represented by “down” arrow); at the same time, the  $H_2$  molecule goes to its *ortho*-state (shown by “up” arrows).

Typical RF-SABRE spectra are shown in Figure 1 together with the thermal NMR spectrum recorded before bubbling the sample with parahydrogen. In the RF-SABRE spectra the phase of the lines depends on the frequency  $\nu_{rf}$ . The enhancements achieved for the

substrate are about 360, which is much higher than the reported high-field SABRE effect<sup>8</sup> based on ‘spontaneous’ (i.e. without RF-excitation) polarization transfer to the substrate. Polarization is formed predominantly on the *ortho*-protons of py; however, small polarization is also seen for other protons. In addition, we observed polarized signals of  $H_2$  in the solvent bulk ( $H_2$ ) and at the catalyst (*c*- $H_2$ ) with opposite sign as compared to those of the *ortho*-protons of py. The signal enhancement for the two  $H_2$  signals is different for different substrates; the highest enhancement achieved when 2,2'-bipyrazine was used as a substrate was about 100-200 for  $H_2$  and about 700 for *c*- $H_2$  (see ESI).

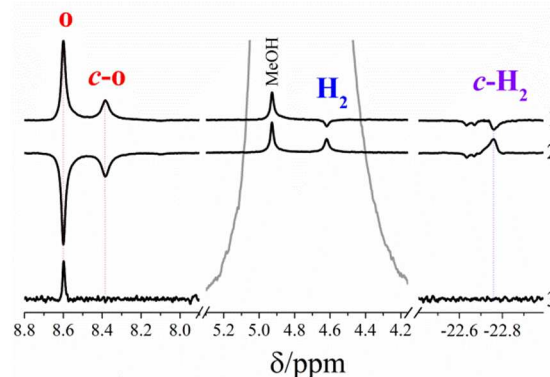


**Figure 1.**  $^1H$  RF-SABRE spectra obtained with the IrMes catalyst after applying an RF-field with amplitude of 28.6 kHz and frequency positions  $\nu_{rf} = -7.0$  ppm (trace 1),  $-7.35$  ppm (trace 2). Deuterated py (proton abundance of 0.5%) was used as a substrate; positions of different protons are assigned. Here *o* and *c-o* denote the *ortho*-protons of py in the bulk and bound to the catalyst;  $H_2$  and *c*- $H_2$  denote dihydrogen in the bulk and at the catalyst, respectively. The thermal NMR spectrum obtained after 128 acquisitions with a  $\pi/2$ -read pulse is also shown for comparison (trace 3).

Let us now give the explanation of the SABRE mechanism and also discuss how the enhancement depends on the parameters of the RF-field. Here we will not go into full detail of the spin dynamics, but provide a descriptive and reasonably simple treatment of the problem under study. Let us write down the Hamiltonian of the spin system under RF-excitation. For simplicity, we assume here that the substrate has only one spin (M-spin) and that the chemical shifts of the protons coming from parahydrogen (AA'-protons) have identical chemical shifts in the complex. This is the minimal spin system, in which the SABRE effect can be formed; it also corresponds to the case of deuterated py having only one proton or only residual protons. Then the Hamiltonian in the rotating frame is:

$$\hat{H}_{rf} = -\delta\nu_A(\hat{I}_{Az} + \hat{I}'_{Az}) - \delta\nu_M\hat{I}_{Mz} + J_{AA'}(\hat{\mathbf{I}}_A \cdot \hat{\mathbf{I}}_{A'}) + J_{AM}(\hat{\mathbf{I}}_A \cdot \hat{\mathbf{I}}_M) + J_{A'M}(\hat{\mathbf{I}}_{A'} \cdot \hat{\mathbf{I}}_M) - \nu_1(\hat{I}_{Ax} + \hat{I}'_{Ax} + \hat{I}_{Mx}) \quad (1)$$

where  $\delta\nu_i$  are the NMR frequencies of spins in the rotating frame;  $J_{ij}$  are the scalar spin-spin interaction constants. Here it is more suitable to take the following terms

$$\hat{V} = J_{AM}(\hat{\mathbf{I}}_A \cdot \hat{\mathbf{I}}_M) + J_{A'M}(\hat{\mathbf{I}}_{A'} \cdot \hat{\mathbf{I}}_M) \quad (2)$$

as a small perturbation into consideration. This is a good approximation when  $J_{AA'}$  is by far the largest coupling in the spin system. The main part of the Hamiltonian,  $\hat{H}_0 = \hat{H}_{rf} - \hat{V}$ , can be most conveniently written in the so-called Doubly Tilted Frame (DTF) where the spins in each group (AA'-protons and M-proton) are quantized along their effective fields in the rotating frame, see Figure 2a. In this frame  $\hat{H}_0$  takes the form:

$$\hat{H}_{0,dtf} = -\nu_{A,dtf}(\hat{I}_{Az} + \hat{I}'_{Az}) - \nu_{M,dtf}\hat{I}_{Mz} + J_{AA'}(\hat{\mathbf{I}}_A \cdot \hat{\mathbf{I}}_{A'}) \quad (3)$$

where  $\nu_{A,dtf} = \sqrt{(\delta\nu_A)^2 + \nu_1^2}$  and  $\nu_{M,dtf} = \sqrt{(\delta\nu_M)^2 + \nu_1^2}$ . In this frame there are two level crossings occurring when<sup>17</sup>

$$\nu_{A,dtf} - \nu_{M,dtf} = \pm J_{AA'} \quad (4)$$

These crossings are between the energy levels corresponding to the state composed of the singlet configuration of the AA'-protons and  $\beta$  of the M-proton,  $|S\beta\rangle$ , and of the lower triplet state of the AA'-protons and  $\alpha$  of the M-proton,  $|T_-\alpha\rangle$ , in the DTF (corresponding to the “+” sign in eqn. 4) or between  $|S\alpha\rangle$  and the upper triplet state of the AA'-protons and  $\beta$  of the M-proton,  $|T_+\beta\rangle$  (corresponding to the “-” sign in eqn. 4); initially only the levels with singlet character of the AA'-spins are populated. At the level crossing points the perturbation term  $\hat{V}$  becomes important: when  $J_{AM} \neq J_{A'M}$  it mixes the states and turns the crossing into an LAC. Consequently, the populations of the involved levels are mixed. When the system is brought to the LAC between the  $|S\alpha\rangle$  and  $|T_+\beta\rangle$  states, see Figure 2b, this kind of mixing results in positive polarization of the AA'-spins along their effective field in the DTF and negative polarization of the M-spin along its effective field in the DTF. For the other LAC (Figure 2c) the resulting polarization is of the same size, but opposite sign for both the AA' and M-protons. This simple model leads to two important consequences: (i) the RF-frequency dependence of polarization is anti-symmetric with respect to the center of the spectrum,  $(\nu_A + \nu_M)/2$ ; (ii) polarization of the AA'-protons ( $H_2$ ) has opposite sign to that of the M-proton belonging to the substrate.

Finally, let us discuss the conditions for having an LAC in the DTF. From eqn. (4) it follows that the two frequencies,  $\nu_{A,dtf}$  and  $\nu_{M,dtf}$ , should have a difference equal to  $\pm J_{AA'}$ , which is achieved when the frequency  $\nu_{rf}$  is placed almost at  $(\nu_A + \nu_M)/2$  having only a small offset from this value (either positive or negative). In addition, to make efficient the mixing of the crossing levels it is required<sup>20</sup> that the angle between the two quantization axes of the DTF,  $\Theta = \theta_A + \theta_M$ , deviates from  $\pi$ , see Figure 2a. This condition is achieved when  $\nu_1$  is sufficiently large, i.e., it is larger than or at least comparable to  $(\nu_A - \nu_M)$ . In this situation in the course of mixing at the LAC regions the spins acquire magnetization along the x-axis in the non-tilted rotating frame, which is detected in our experiments.

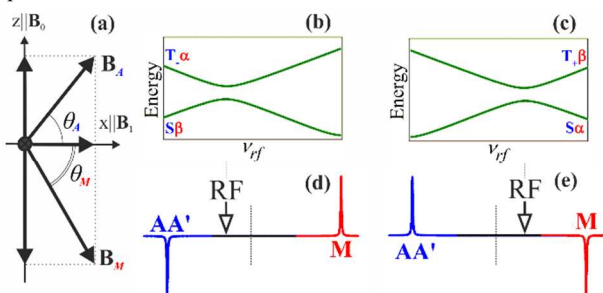


**Figure 2.** Schematic representation of the axes of the doubly tilted frame (DTF) (a): spins are quantized along the new axes,  $\mathbf{B}_A$  and  $\mathbf{B}_M$ ; they are inclined with respect to the x-axis, the inclination angles being  $\theta_A$  and  $\theta_M$ . In (b) and (c) we show the LACs in the DTF between the levels  $|S\beta\rangle$  and  $|T_-\alpha\rangle$  and between the levels  $|S\alpha\rangle$  and  $|T_+\beta\rangle$ . In (d) and (e) the NMR spectrum resulting from spin mixing at each LAC (with the position of the applied RF-field indicated by an arrow) is shown under the corresponding energy diagram.

The spectra 1 and 2 shown in Figure 1 are taken when the LAC conditions are exactly fulfilled. The RF-frequency  $\nu_{rf}$  is chosen such that it is placed almost at the ‘center of the spectrum’, that is, at  $\nu_{rf} = (\nu_{cH_2} + \nu_0)/2$ , (here  $\nu_0$  stands for the NMR frequency of the ortho-protons of equatorial py in the active complex) but is slightly detuned from this value. Positive and negative offsets result in different sign of polarization of the ortho-protons and  $c\text{-H}_2$  and  $H_2$ , in full accordance with our theoretical treatment, (compare curves 1

and 2). When the RF-frequency is such that the system stays away from an LAC the SABRE effect vanishes.

The full dependence of the high-field SABRE effect on the RF-field frequency is shown in Figure 3 for the complex with the IrIMes catalyst. It is clearly seen that placing the frequency at the ‘center of the spectrum’ gives no polarization; however, there are positive and negative peaks in the  $\nu_{rf}$ -dependence, at which the substrate is efficiently polarized, see Figure 3a. The same shape of the frequency dependence is also found for  $H_2$  and  $c\text{-H}_2$ , but with the opposite phase, see Figure 3b. The frequency dependences are in good agreement with the calculation. Details of the calculation method and the NMR parameters used in the calculation are also given in ESI. Analogous results are seen for RF-SABRE obtained with Crabtree’s catalyst and also for RF-SABRE obtained with other substrates (see ESI).

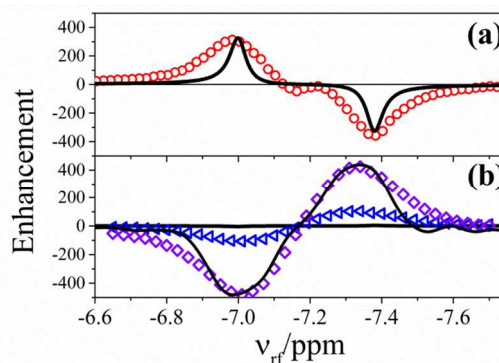


**Figure 3.** Dependence of the RF-SABRE-induced NMR enhancement on  $\nu_{rf}$  for (a) the ortho-protons of free deuterated py (proton abundance is 0.5%) and for (b)  $H_2$  (blue triangles) and  $c\text{-H}_2$  (violet diamonds) when protonated py was used as a substrate. The RF-SABRE effect was observed with the IrIMes catalyst; lines show the simulation results.

RF-SABRE signal enhancements are summarized in Chart 1. It is seen that the effect is not limited solely to py with only one proton but is more general. Using the same physical principles it is possible to polarize other molecules containing a nitrogen atom in the aromatic ring. In fully protonated py the enhancement decreases but is still substantial; for fully protonated 2,2'-bipyrazine the enhancement is about 200. In other cases the NMR enhancement is larger than that given by the pure cross-relaxation mechanism. Thus, despite the more complex spin dynamics in systems with several protons, it is feasible to achieve the RF-SABRE effect. Its dependence on the key experimental parameters, RF-field amplitude and frequency, is discussed in more detail in ESI.

## Conclusions

To summarize, we have proposed a method to perform RF-SABRE experiments at high magnetic field. The method exploits mixing of spin states at LACs; the LAC conditions are fulfilled by turning on a strong RF-field with properly chosen amplitude and frequency. By varying the RF frequency one can also vary the phase of polarized NMR signals in a desirable way. These results can be well accounted for by the theoretical treatment described; also a simple semi-qualitative explanation of our observations is given that is based on spin mixing in the doubly tilted frame of reference.

With the signal enhancement around 360, it is a significant step forward for establishing SABRE as a high-field technique. The method is relatively straightforward in use and only requires careful setting of the RF-field parameters. Since carrying out experiments at high magnetic fields is technically much easier than field-cycling and requires only standard NMR equipment we anticipate that our

method will give access to exciting applications in NMR spectroscopy and imaging providing a permanent source of nuclear hyperpolarization. Thus, the feasibility of high-field SABRE experiments opens new avenues in exploiting hyperpolarized spins.

### Acknowledgements

This work was supported by the Russian Science Foundation (grant No. 14-13-01053). H.M.V. is thankful to the Alexander von Humboldt Foundation for financial support. We acknowledge Dr. Pavel Petrov for providing us with the IrMesCODCl pre-catalyst.

### Notes and references

<sup>a</sup> International Tomography Center, Siberian Branch of the Russian Academy of Science, Institutskaya 3a, Novosibirsk, 630090, Russia. E-mail: [ivanov@tomo.nsc.ru](mailto:ivanov@tomo.nsc.ru); Tel.: +7(383)330-8868; Fax: +7(383)333-1399

<sup>b</sup> Novosibirsk State University, Pirogova 2, Novosibirsk, 630090, Russia.

<sup>c</sup> Institut für Experimentalphysik, Freie Universität Berlin, Arnimallee 14, Berlin, 14195, Germany.

Electronic Supplementary Information (ESI) available: Details of sample preparation; calculation algorithm; results for Crabtree's catalyst and other substrates; NMR parameters of the spin systems. See DOI: 10.1039/c000000x/

1. R. W. Adams, J. A. Aguilar, K. D. Atkinson, M. J. Cowley, P. I. Elliott, S. B. Duckett, G. G. Green, I. G. Khazal, J. Lopez-Serrano and D. C. Williamson, *Science*, 2009, **323**, 1708-1711.
2. R. W. Adams, S. B. Duckett, R. A. Green, D. C. Williamson and G. G. Green, *J. Chem. Phys.*, 2009, **131**, 194505.
3. K. D. Atkinson, M. J. Cowley, P. I. P. Elliott, S. B. Duckett, G. G. R. Green, J. López-Serrano and A. C. Whitwood, *J. Amer. Chem. Soc.*, 2009, **131**, 13362-13368.
4. M. J. Cowley, R. W. Adams, K. D. Atkinson, M. C. R. Cockett, S. B. Duckett, G. G. R. Green, J. A. B. Lohman, R. Kerssebaum, D. Kilgour and R. E. Mewis, *J. Am. Chem. Soc.*, 2011, **133**, 6134-6137.
5. E. B. Dücker, L. T. Kuhn, K. Münnemann and C. Griesinger, *J. Magn. Reson.*, 2012, **214**, 159-165.
6. M. Fekete, O. Bayfield, S. B. Duckett, S. Hart, R. E. Mewis, N. Pridmore, P. J. Rayner and A. Whitwood, *Inorg. Chem.*, 2013, **52**, 13453-13461.
7. N. Eshuis, N. Hermkens, B. J. A. van Weerdenburg, M. C. Feiters, F. P. J. T. Rutjes, S. S. Wijmenga and M. Tessari, *J. Am. Chem. Soc.*, 2014, **136**, 2695-2698.
8. D. A. Barskiy, K. V. Kovtunov, I. V. Koptyug, P. He, K. A. Groome, Q. A. Best, F. Shi, B. M. Goodson, R. V. Shchepin, A. M. Coffey, K. W. Waddell and E. Y. Chekmenev, *J. Am. Chem. Soc.*, 2014, **136**, 3322-3325.
9. J.-B. Hövener, N. Schwaderlapp, T. Lickert, S. B. Duckett, R. E. Mewis, L. A. R. Highton, S. M. Kenny, G. G. R. Green, D. Leibfritz, J. G. Korvink, J. Hennig and D. von Elverfeldt, *Nature Commun.*, 2013, **4**, 2946.
10. J. Natterer and J. Bargon, *Prog Nucl Mag Res Sp*, 1997, **31**, 293-315.
11. K. Miesel, K. L. Ivanov, A. V. Yurkovskaya and H.-M. Vieth, *Chem. Phys. Lett.*, 2006, **425**, 71-76.

12. A. S. Kiryutin, A. V. Yurkovskaya, R. Kaptein, H.-M. Vieth and K. L. Ivanov, *J. Phys. Chem. Lett.*, 2013, **4**, 2514-2519.
13. A. N. Pravdivtsev, A. V. Yurkovskaya, R. Kaptein, K. Miesel, H.-M. Vieth and K. L. Ivanov, *Phys. Chem. Chem. Phys.*, 2013, **15**, 14660-14669.
14. L. Buljubasich, M. B. Franzoni, H. W. Spiess and K. Münnemann, *J. Magn. Reson.*, 2012, **219**, 33.
15. M. B. Franzoni, D. Graafen, L. Buljubasich, L. M. Schreiber, H. W. Spiess and K. Münnemann, *Phys. Chem. Chem. Phys.*, 2013, **15**, 17233-17239.
16. K. L. Ivanov, A. N. Pravdivtsev, A. V. Yurkovskaya, H.-M. Vieth and R. Kaptein, *Prog. Nucl. Magn. Reson. Spectrosc.*, 2014, **81**, 1.
17. A. N. Pravdivtsev, A. V. Yurkovskaya, H.-M. Vieth, K. L. Ivanov and R. Kaptein, *ChemPhysChem*, 2013, **14**, 3327-3331.
18. J.-B. Hövener, S. Knecht, N. Schwaderlapp, J. Hennig and D. von Elverfeldt, *ChemPhysChem*, 2014, **15**, 2636.
19. R. H. Crabtree, M. Lavin and L. Bonneviot, *J. Am. Chem. Soc.*, 1986, **108**, 4032.
20. A. N. Pravdivtsev, A. V. Yurkovskaya, N. N. Lukzen, H.-M. Vieth and K. L. Ivanov, *Phys. Chem. Chem. Phys.*, 2014, **16**, 18707.

### Graphical Abstract

